Power Modeling of a Skid Steered, Wheeled Robotic Ground Vehicle

Oscar Chuy Jr., Emmanuel Collins Jr., Wei Yu, and Camilo Ordonez

***Abstract*— Analysis of the power consumption of a robotic ground vehicle (RGV) is important for planning since it enables motion plans that do not violate the power limitations of the motors, energy efficient path planning, prediction of the ability to complete a task based upon the vehicles's current energy supply, and estimation of when the vehicle will need to refuel or recharge. Power modeling is particularly difficult for skid steered vehicles because of the complexities of properly taking into account the skidding that is used for vehicle turning. This paper begins with a 2-dimensional, second order differential equation of a skid steered, wheeled RGV and shows that the power model is terrain dependent and is a function of both the turning radius and linear velocity of the vehicle. This model is verified experimentally, and a comprehensive set of experiments was performed to describe the power consumption of a skid steered RGV on asphalt.**

I. Introduction

Many robotic ground vehicles (RGVs) are developed for outdoor tasks and missions that require high levels of autonomy. They can be used in applications such as search and rescue, exploration, surveillance, agriculture, mining, etc. In practice, an important ability for motion planning and successful task completion is the ability to predict power consumption. In particular the development of vehicle power models aids in four important areas of robot motion planning:

1) *Motion planning that avoids vehicle immobilization by taking into account vehicle power limitations.* For example, it will enable the planner to avoid commanded velocity and turn radius combinations that are not executable. This is especially important as the speed of autonomously operating RGVs increases.
2) *Energy efficient path planning.*
3) *Prediction of the ability to complete a task based upon the vehicle's current energy supply.*
4) *Estimation of when to refuel or recharge.*

Power models are especially important for outdoor vehicles, which are often Ackerman steered or skid steered. This paper addresses power modeling for wheeled (as opposed to tracked), skid steered vehicles, which require a more complex theoretical and experimental modeling processes due to the difficulty in modeling the power consumption due to turning by skidding.

Prepared through collaborative participation in the Robotics Consortium sponsored by the U. S. Army Research Laboratory under the Collaborative Technology Alliance Program, Cooperative Agreement DAAD 19-01-2-0012. The U. S. Government is authorized to reproduce and distribute reprints for Government purposes notwithstanding any copyright notation thereon.

O. Chuy, E. Collins, W. Yu are with the Center for Intelligent Systems, Control and Robotics (CISCOR) of the Department of Mechanical Engineering, Florida AM University-Florida State University, Tallahassee, Fl 32310, USA {chuy,ecollins,yuwei,camilor}@eng.fsu.edu

Research related to power and energy consumption of RGVs is reported in [1], [2]. These works do not develop explicit power models, but instead determine energy-efficient trajectories. Ref. [2] focuses on straight line motion of a skid steered RGV. This paper does not explicitly deal with more general (curved) motion and the lack of explicit power models means that this result is not applicable to three of the four capabilities enumerated above.

The research presented in [3], [4] does develop explicit power models for a differentially steered vehicle moving in a straight line. It mentions that power models for general motion can be derived from these results by assuming pure rolling. However, this assumption, though reasonable for differentially steered vehicles, is clearly invalid for skid steered vehicles.

Ref. [7] does consider power modeling of a skid steered tracked vehicle. The power consumption is expressed in terms of the velocities of the left and right wheels. This research essentially assumes that the power consumption is linearly proportional to the linear and angular velocity of the vehicle, where the proportionality constants respectively represent the longitudinal resistance and moment of turning resistance and are assumed to be independent of the turning radius. However, analysis in [5], [6] clearly shows that the moment of turning resistance varies with the turning radius and can be considered constant only for a fixed turning radius. Furthermore, the experiments presented in [7] yield power model curves that are valid for only a small range of turning radii (which enables the experimental results to appear to satisfy the above assumption of turning radius independence). Hence, the presented power model curves capture only a relatively small portion of the overall power model.

This paper describes a power modeling process for a skid steered wheeled vehicle that, unlike the approach of [7], begins with a standard second order differential equation of the vehicle. Hence, this approach involves the intermediate development of a dynamic model of the vehicle that may be used for other planning problems that require a dynamic model, for example, steep hill climbing. Because of this, it is able to capture the interesting braking phenomena of the inner wheels when the turning radius is sufficiently small, a phenomena reproduced by the analytical modeling of [5], [6], which develops a general theory for the motion of *tracked*, skid steered vehicles on firm ground. The power model curves are explicitly in terms of linear velocity and turning

radius, which is convenient for planning.[1] In comparison to [3], [4] this approach reduces the number of experiments required to obtain the straight line power model since it is known a priori that the power vs. velocity curves are straight lines.

The most complete power model curves, which are given in Section , are developed for asphalt terrains. However, power models are inherently terrain dependent and this terrain dependence is seen in some of the earlier power model curves of Section III. Hence, for general outdoor use these models must be developed for each of the terrains that the vehicle is expected to traverse.

It should be mentioned that experiments that developed curves of motor current vs. rate of turn (MCR) are described in [8]. The MCR curves are similar to the torque vs. turning radius curves of this paper. However, the purpose of their development was to characterize terrain trafficability. Although the authors do mention that power prediction can be made using MCR curves, this analysis is not actually pursued.

This paper is organized as follows. Section II presents basic concepts needed for the development of detailed power modeling of a skid steered vehicle and in the process presents experimental results on power analysis for straight line motion. Section III then presents and discusses detailed power model curves for the experimental platform on asphalt. Finally, Section IV summarizes the results and discusses future research.

II. Motion Power Analysis of a Wheeled Skid Steered Vehicle

This section presents basic concepts for power analysis of a wheeled, skid steered vehicle moving in general motion. It begins by describing the experimental vehicle used in this research and then presents and discusses the terms in a general dynamic model of a skid steered vehicle. Next, this model is used to discuss basic concepts in power modeling. Then, to illustrate some of these concepts, experimental results are given for power modeling for the case of straight line motion. The form of the curves for curved motion are then discussed under the assumption of perfect rolling. This leads to the correct form of the power curves.

A. Experimental Platform

As shown in Fig. 1, the experimental platform used in this study was a modified PIONEER 3-AT. It is an outdoor mobile robot and weighs 30 kg. It was modified to run on the QNX realtime operations system with a control sampling rate of 1K Hz. The mobile robot can be commanded with linear velocity and turning radius, or linear and angular velocity at the same rate as the control loop. This removes a practical hardware limitation as mentioned in [8]. The ability to input high command rates allows the robotic ground vehicle to more precisely follow smooth trajectories, which is an important feature to reduce energy expenditure during acceleration and deceleration discussed in [2].

In order to experimentally determine the power consumption of the vehicle, current and voltage sensors were installed at the power supply, and the output of the two motor drivers. This setup allows determination of the total power consumption, which was composed of the motion power, and the computing and sensing power consumption. The motion power consumption was monitored through the motor drivers. It should be noted that the experimental vehicle was driven by four motors, two in each side connected in parallel, and each pair of motors was driven by a motor driver. The computing and sensing power can be derived by subtracting the motion power from the total power.

B. Vehicle Dynamics

Following [9], consider the vehicle dynamics of a wheeled, skid steered vehicle, expressed in the vehicle coordinates, and given by the 2-dimensional, second-order differential equation,

$$\mathbf{M}\ddot{\mathbf{q}} + \mathbf{C}(\mathbf{q}, \dot{\mathbf{q}}) + \mathbf{G}(\mathbf{q}) = \tau, \tag{1}$$

where the coordinates $\mathbf{q}$ are chosen such that $\dot{\mathbf{q}} = [v\ \omega]^T$ with v and ω respectively the vehicle's linear velocity and angular velocity about the vertical axis of the body-centered vehicle axes, $\tau = [F\ M]^T$ with F and M respectively the applied force and torque about the vertical axis of the body-centered vehicle axes, $\mathbf{M}$ is the inertia matrix, $\mathbf{C}(\dot{\mathbf{q}}, \mathbf{q}) = [F_R\ M_R]$ with F_R and M_R respectively the longitudinal resistance and the moment of resistance about the vertical axis of the body-centered vehicle axes, and $\mathbf{G}(\mathbf{q})$ is the gravitational term. The first and third terms in (1) can be derived analytically. However, the terrain dependent, second term $\mathbf{C}(\mathbf{q}, \dot{\mathbf{q}})$ is very difficult to determine through analysis based purely on physics. The approach of this paper is to describe the force and torque associated with $\mathbf{C}(\mathbf{q}, \dot{\mathbf{q}})$ by experimentally determined curves. Note that even the complex theoretical analysis of [5], [6], which attempts to describe $\mathbf{C}(\mathbf{q}, \dot{\mathbf{q}})$ analytically for tracked, skid steered

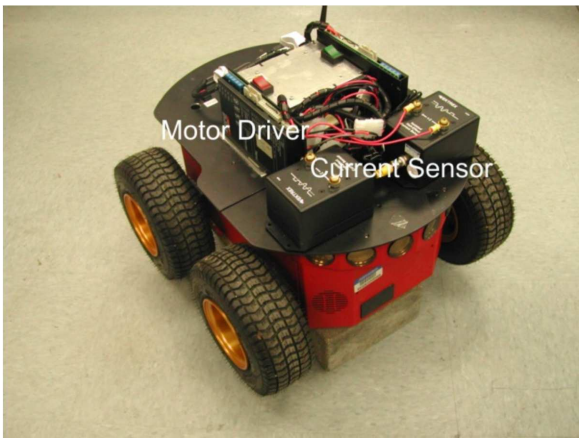

Fig. 1. Experimental Vehicle : Modified PIONEER 3-AT installed new control system and power monitoring sensors

[1](Note that the angular velocity ω is related to the linear velocity v and the turning radius r by $\omega = \frac{v}{r}$.)

vehicles requires experimentation to determine three key, terrain dependent, parameters of the derived model (rolling resistance, coefficient of friction and sheer modulus).

C. Power Analysis Preliminaries

Given a desired vehicle trajectory $(\mathbf{q_d}, \dot{\mathbf{q}}_\mathbf{d}, \ddot{\mathbf{q}}_\mathbf{d})$ the corresponding force/torque vector can be determined based on (1) and is given by

$$\tau_\mathbf{d} = \mathbf{M}\ddot{\mathbf{q}}_\mathbf{d} + \mathbf{C}(\mathbf{q_d}, \dot{\mathbf{q}}_\mathbf{d}) + \mathbf{G}(\mathbf{q_d}). \tag{2}$$

The power P required to track the trajectory is then given as

$$P = \dot{\mathbf{q}}_\mathbf{d}{}^\mathrm{T}\tau_\mathbf{d}. \tag{3}$$

Substituting (2) into (3) then yields

$$P = \dot{\mathbf{q}}_\mathbf{d}^\mathrm{T}\mathbf{M}\ddot{\mathbf{q}}_\mathbf{d} + \dot{\mathbf{q}}_\mathbf{d}{}^\mathrm{T}\mathbf{C}(\mathbf{q_d}, \dot{\mathbf{q}}_\mathbf{d}) + \dot{\mathbf{q}}_\mathbf{d}{}^\mathrm{T}\mathbf{G}(\mathbf{q_d}). \tag{4}$$

From earlier discussion of (1) it follows that the first and third terms on the right hand side of (4) can be determined analytically. In this paper it is assumed that the vehicle moves on a flat surface such that the third term is zero. The second term, which is the power consumption due to rolling resistance and the moment of turning resistance, dominates the first term for long distance travel in which the vehicle's velocity does not frequently vary. The focus of this paper is on experimentally obtaining power curves to describe this term. These curves are obtained by commanding the vehicle with constant linear velocities and constant turning radii on flat ground. It should be mentioned that a practical path tracking algorithm normally commands the vehicle with constant velocity while changing the instantaneous center of rotation to track the path as discussed in [10], [11]. This essentially views a given path as a series of circular motions of various radii and enables the results developed in this paper to be applied to general motion.

Define P_R to be the second term on the right hand side of 4, i.e.,

$$P_R = \dot{\mathbf{q}}_\mathbf{d}^\mathrm{T}\mathbf{C}(\mathbf{q_d}, \dot{\mathbf{q}}_\mathbf{d}). \tag{5}$$

Then, since $\dot{\mathbf{q}}^T = [v\ \omega]$ and $\mathbf{C}(\mathbf{q}, \dot{\mathbf{q}}) = [F_R\ M_R]$,

$$P_R = F_R v + M_R \omega. \tag{6}$$

The velocity dependence of $\mathbf{C}(\mathbf{q}, \dot{\mathbf{q}})$ is negligible at low speeds as discussed in [5].

D. Power Model Curves for a Skid Steered Vehicle in Straight Line Motion

The assumption of pure rolling is a reasonable one for wheeled skid steered vehicles in straight line motion. Since $\omega = 0$ in this case, it follows from (6) that

$$P_R = F_R v, \tag{7}$$

and hence the power is dependent on the terrain dependent, longitudinal resistance F_R.

Experiments were performed on four terrains (asphalt, gravel, grass and sand) to show the terrain dependent relationship between power P_R and velocity v. For each terrain, a set of command velocities $\{v_{d,1}, v_{d,2}, \ldots, v_{d,k}\}$ was considered. Each experiment on a given terrain applied one of these command velocities $v_{d,i}$ to the robot for 10 sec. and the resulting power consumption P_R was measured.

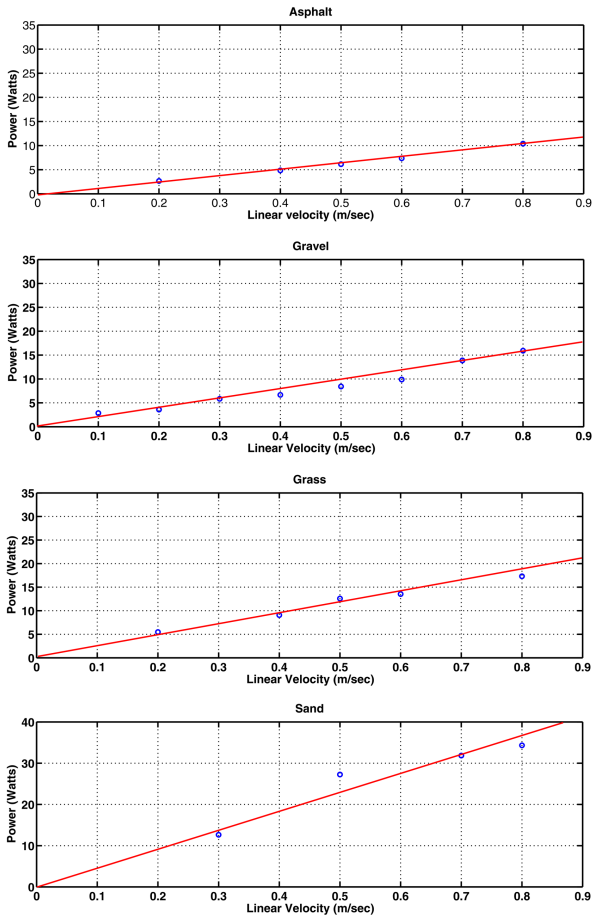

Fig. 2. Preliminary experiments on power consumption of a robotic ground vehicle on asphalt, gravel, grass, and sand in straight line motion.

The power vs. velocity curves for the four terrains are shown in Fig. 2, and, as expected, each of the curves shows a linear relationship between power and velocity. However, the slope of this linear relationship varies with the terrain. In fact, the terrain curves are given from top to bottom in order of increasing slope (i.e., power consumption). It should be noted that the power displayed in Fig. 2 is for a single drive system (left wheels) and the total motion power can be determined by adding left and right drive systems, which would essentially double the slopes of the curves.

E. Analysis of Curved Motion Assuming Pure Rolling

It is important to extend the analysis of vehicle power consumption to curved motion. Below, we perform a preliminary analysis under the assumption of pure rolling. This assumption can be reasonably applied to an Ackermann steered vehicle or a differentially steered vehicle, which have some wheels that are passive and used for balancing. However, this assumption is invalid for skid steered vehicles. In this paper, the results of this analysis is used as an

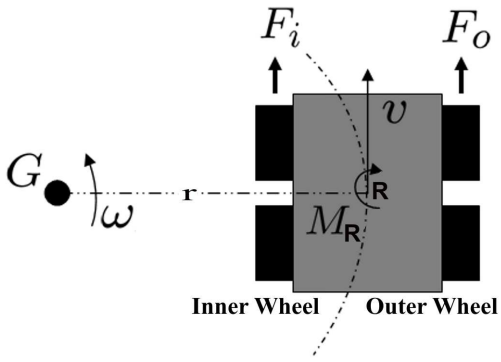

Fig. 3. Representation of wheeled skid steering vehicle force/torque and moment of turning resistance during curving

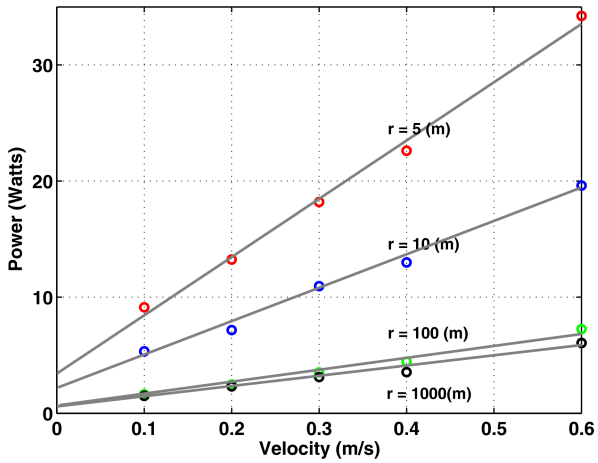

Fig. 4. Power versus velocity for different turning radius.

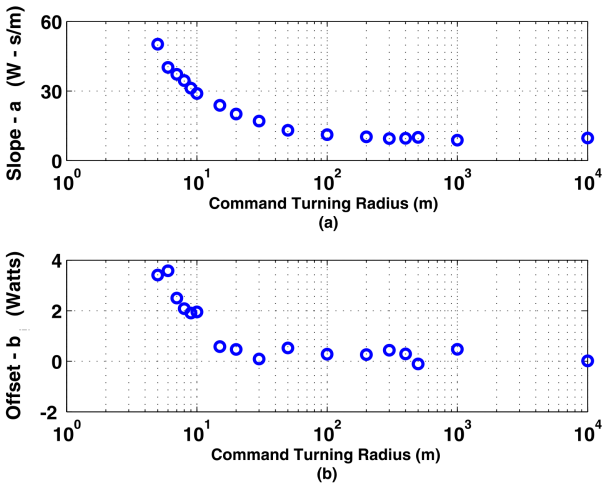

Fig. 5. Preliminary experiment result on the coefficient of the power model. (a) slope of the power model (b) offset of the power model.

intermediate step in the analysis of power consumption for skid steered vehicles in curved motion.

As shown in Fig. 3, consider a skid steered wheeled vehicle moving in circular motion of radius r about point G with a linear velocity v and an angular velocity of ω. In Fig. 3 F_i and F_o denote respectively the force of the inner and outer wheels. M_R denotes the moment of resistance that under the assumption of pure rolling is purely due to the longitudinal resistances. It follows that under constant linear and angular velocity

$$F_R = F_o + F_i, \tag{8}$$

$$M_R = \frac{B}{2}(F_o - F_i). \tag{9}$$

Substituting (8) and (9) into (6) and recognizing that $w = v/r$ shows that the power consumption is the function of r and v given by,

$$P(r, v) = a(r)v, \tag{10}$$

where

$$a(r) = (F_o + F_i) + \frac{B}{2}(F_o - F_i)\frac{1}{r}. \tag{11}$$

Equations (10) and (11) show that, as would be expected, the effect of the moment of turning resistance decreases as the turning radius r increases.

F. Power Model of Skid Steered Wheeled Vehicle in Curved Motion

The motion power consumption described by (10) was derived under the assumption of pure rolling and hence does not capture the effects of skidding. Here, it is assumed that the actual power consumption is given by

$$P(r, v) = a(r)v + b(r), \tag{12}$$

where from (11) it is assumed that for $r_2 > r_1$ $a(r_2) < a(r_1)$ and the term $b(r)$ has been added to take into account the effects of skidding and satisfies $\lim_{r\to\infty} b(r) = 0$, i.e., it is negligible for straight line motion.

Preliminary sets of experiments were conducted on a vinyl tile to verify (12). In each set of experiments the command turning radius was fixed. Then, in each of the experiments within that set, the vehicle was then commanded to move for 10 sec. at a given velocity. The results are shown in Fig. 4, which clearly verify (12), i.e., for each turn radius the power consumption increases linearly with velocity and there is an offset that varies with the turn radius. Also, as expected, as the turning radius increases, the slope of the power vs. velocity curves decreases and the offset also decreases. Figs. 5(a) and 5(b) show respectively $a(r)$ vs. r and $b(r)$ vs. r. It follows that for a given terrain, the power consumption can be estimated by experimentally obtained estimates of $a(r)$ and $b(r)$.

III. Comprehensive Experimental Results for Motion on Asphalt

Comprehensive experiments were performed for the experimental vehicle's movement on asphalt. These experiments consisted of a set of experiments in which the vehicle was commanded with a linear velocity v_d and a turning radius r_d, represented by **cmd**(v_d, r_d). This

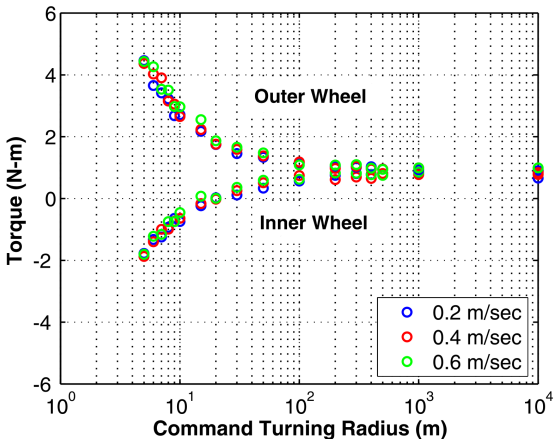

Fig. 6. Torque versus command turning radius. The outer wheel shows propulsion and inner wheel exhibits braking on small turning radius. Both outer and inner wheel torques converge to the same value, which is the longitudinal resistance times the wheel radius.

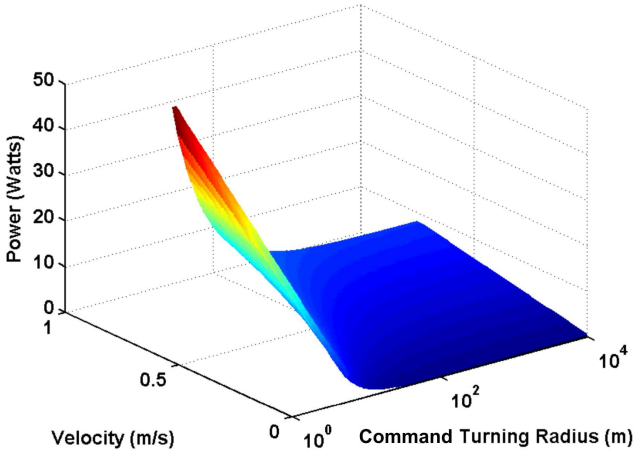

Fig. 7. Outer wheel power surface on asphalt for different velocity and turning radius.

basic experiment was performed for all combinations of v_d and r_d in the sets $\{0.1, 0.2, 0.3, 0.4, 0.6\}\mathrm{m/s}$ and $\{5, 6, 7, 8, 9, 10, 15, 20, 30, 50, 100, 200, 300, 400, 500, 1000, 10000\}\mathrm{m}$.

Plots of wheel torque vs. turning radius for both inner and outer wheels are shown in Fig. 6 for three of the five velocities.These curves are seen to be essentially independent of the velocity. Also, notice that at sufficiently small turning radii (approximately less than 2m), the inner wheel shows braking while the outer wheel exhibits propulsion. In addition, it is seen that a large force/torque was needed for small turning radii. A zero turning radius was not considered in the experiments due to a power constraint on the vehicle motors, which led to vehicle immobilization when a zero turning radius was commanded.

Wheel torque vs. turning radii curves are also developed via theoretical analysis in [5] for skid steered *tracked* vehicles. The results of [5] were verified with published experimental results, but this correlation required careful tuning of three parameters, rolling resistance, coefficient of friction, and shear modulus, the latter which is particularly difficult to measure. The curves in Fig. 6 appear identical in form to those of [5]. The research reported here found that that the curves for the inner and outer wheels can be fit with an exponentially decaying function of the form,

$$T(r) = T_\infty + T_\alpha e^{-\beta \log(r+1)} \tag{13}$$

where $T_\infty = T(r)$ as $\lim_{r\to\infty}$ and α and β are also model dependent constants. Curves such as those shown in Fig. 6 can be used to define the term $\mathbf{C}(\mathbf{q}, \dot{\mathbf{q}})$ in (1). Once we know the wheel torque, the power consumption can easily be determined by multiplying this torque with the angular velocity of the wheel. However, power loss due to skidding cannot be captured with this approach.

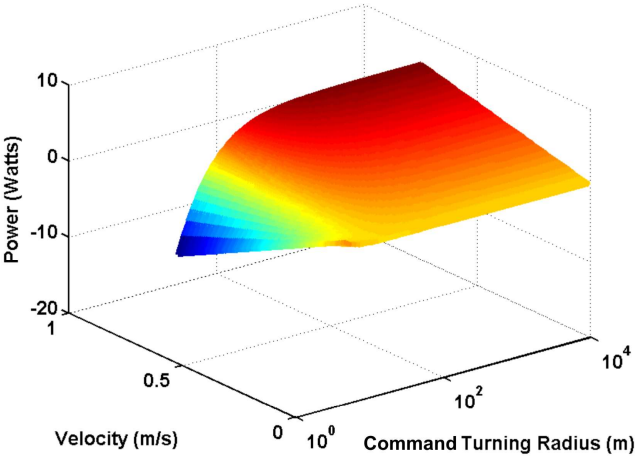

Fig. 8. Inner wheel power surface on asphalt for differen velocity and turning radius.

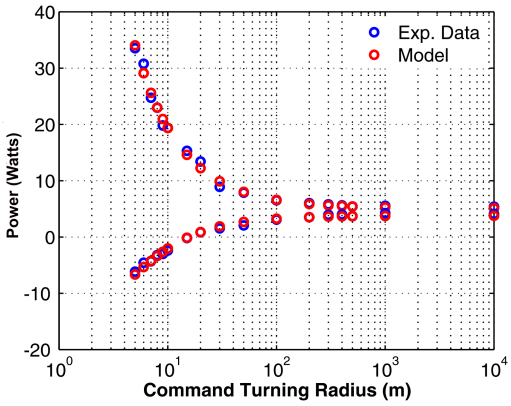

Fig. 9. Power model evaluation on asphalt. The command velocity was 0.5 m/s several command turning radius were considered.

A. Power Modeling Curves for Curved Motion

Recall that we have already shown that the power model can be represented in the form (12). Furthermore, this

research has found that $a(r)$ and $b(r)$ can be represented by the same functional form of the wheel torques in (13), that is

$$a(r) = a_\infty + a_\alpha e^{-a_\beta \log(r+1)} \quad (14)$$

$$b(r) = b_\infty + b_\alpha e^{-b_\beta \log(r+1)} \quad (15)$$

Based on the power data taken from the experiments, the parameters of the power model described in (14)-(15) were determined using a MATLAB optimization function called `lsqnonlin`. These parameters were determined such that the sum of the error square between the model and the actual power data was minimum. The parameters of the power model for both inner and outer wheels are shown in Table I. In addition, the parameters of the power model used in the preliminary experiments as mentioned in Sec. II are shown in Table II.

Power surfaces for the inner and outer wheels were created as a function of command linear velocity and turning radius, and these are shown shown in Fig. 7 and Fig. 8. These power surfaces describe the operating power of the inner and outer wheel drive systems for a large range of linear velocity and turning radii. These surfaces can be used to determine whether a commanded vehicle velocity and turning radius violate the power limits of the vehicle.

Negative power is sometimes associated with the inner wheel while the power of the outer wheel is always positive. However, it should be recognized that the negative power still drains energy from the battery. Hence the negative sign simply means that the direction of the applied torque is opposite to the direction of motion.

TABLE I
POWER MODEL PARAMETERS (ASPHALT)

	a_∞	b_α	a_β	b_∞	b_α	b_β
Inner Wheel	7.5313	-170	2.5507	0.006	500	7.7136
Outer Wheel	10.2208	250	2.2187	0.03397	300	4.818

TABLE II
POWER MODEL PARAMETERS (VINYL FLOOR)

	a_∞	b_α	a_β	b_∞	b_α	b_β
Inner Wheel	7.2772	-100	2.0404	-0.004	250	7.0894
Outer Wheel	9.8043	300	2.6260	0.01263	35.32	2.9796

B. Evaluation of the Power Model Curves

The power model of the robotic ground vehicle on asphalt was evaluated by considering a constant command velocity for various turning radii Fig. 9 shows the power evaluation with a command velocity of 0.5 m/s for several turning radii. The results show a similar power trend as turning radius was increased. Table III shows the mean of absolute error for command velocity $\{0.25\ 0.5\ 0.75\}$m/s. It should be noted that the command velocities on the evaluation were not used on the modeling. The evaluation results clearly show the validity of the power model.

TABLE III
POWER EVALUATION ON ASPHALT BASED ON (MAE) MEAN OF ABSOLUTE ERROR

Linear Vel. (m/s)	0.25	0.50	0.75
MAE Inner Wheel	0.28 (W)	0.29 (W)	0.45 (W)
MAE Outer Wheel	0.47 (W)	0.48 (W)	0.85 (W)

C. Application of the Power Model Curves

The experimental robotic ground vehicle used in this study had a maximum linear velocity of 0.9 m/s on asphalt. Hence, a command from a path planner of 0.4 m/s and a turning radius of 2 (m), which will be denoted as **`cmd`**(0.4,2.0) should not pose any problem based on the velocity limit of the vehicle. In the implementation of **`cmd`**(0.4,2.0), it was observed that the vehicle was way off with respect to the desired path. Fig. 10 shows the outer wheel power surface and the power limit. It can be observed that the command **`cmd`**(0.4,2.0) violates the power limit of the vehicle and leads to torque saturation. Fig 11 shows the actual and commanded linear velocity of the vehicle.

In practice, a path planner can incorporate power models to determine executable command velocity and turning radius for the vehicle, which yield vehicle power consumption within the power limits. In addition, it should be noted that a vehicle has a different maximum velocity for each terrain and should be incorporated to the path planner using models. The aforementioned example clearly shows that the kinematic model is not enough to plan outdoors.

IV. CONCLUSION

Beginning with a standard vehicle model, this paper presented an approach for experimentally developing the power model of a skid steered, wheeled RGV. The model characterizes the power consumption of the inner and outer wheels in terms of the linear velocity and turning radius of the RGV. The power model was used to determine combinations of linear velocity and turning radius that violate the power limitations of an RGV actuator, which can lead to unexpected vehicle behavior. The power model is terrain dependent and hence the power curves will differ for the vehicle's motion on different terrains.

Future work will use the power models for energy efficient path planning. Another goal of future research is to reduce

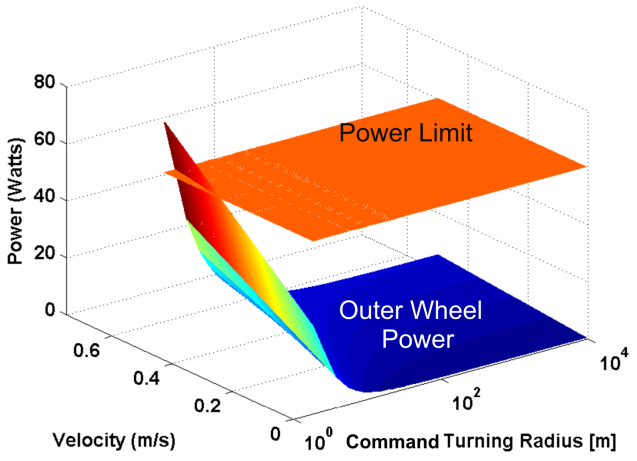

Fig. 10. Power surface of the outer wheel and the power limit of the outer wheel drive system.

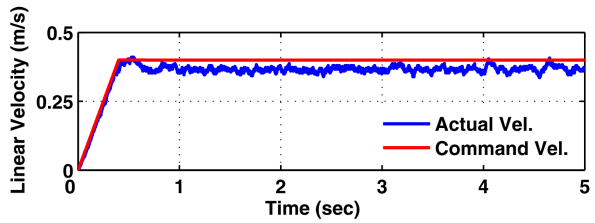

Fig. 11. Command and actual linear velocity of the vehicle for `cmd` (0.4,2)

the number of experiments that are needed to develop the power models.

REFERENCES

[1] A. Barili and M. Ceresa and C. Parisi, "Energy Saving Motion Control for an Autonomous MObile Robot", Proceedings of the 1995 IEEE International Symposium on Industrial Electronics, pp. 674-676, July 1995.

[2] C.H. Kim and B. K. Kim,"Minimum-Energy Translational Trajectory Generation for Differential-Driven Wheeled Mobile Robots", Journal of Intelligent Robot System, pp. 367-383, 2007.

[3] Y. Mei and Y.H. Lu and Y. C. Hu and C.S. George Lee, "Deployment of Mobile Robots with Energy and Timing Constraints", IEEE Transactions on Robotics, pp. 507-522, June 2006.

[4] Y. Mei and Y.H. Lu and C.S. George Lee and Y. C. Hu, "Energy-Efficient Mobile Robot Exploration", Proceedings of the 2006 IEEE International Conference on Robotics and Automation, pp. 505-511, Orlando, Florida, May 2006.

[5] J.Y. Wong, " Theory of Ground Vehicle", John Wiley & Sons, Inc. 2001.

[6] J.Y. Wong and C.F. Chiang,"A General Theory for Skid Steering of Tracked Vehicles on Firm Ground", Proceedings of the Institution of Mechanical Engineers, Part D, Journal of Automotive Engineering, Vol. 215, No. D3, pp. 343-355, 2001.

[7] J. Morales and J. L. Martinez and A. Mandow and A. Garcia-Cerezo and J. Gomez-Gabriel and S. Pedraza, "Power Anlysis for a Skid-Steered Tracked Mobile Robot", Proceeding of the 2006 IEEE International Conference on Mechatronics, pp. 420-425, July 2006.

[8] L. Ojeda and J. Borenstein and G. Witus and R. Karlsen, "Terrain Characterization and Classification with a Mobile Robot", Journal of Field Robotics, pp. 103-122, 2006.

[9] K Kozlowski and D Pazderski, "Modeling and Control of a 4-Wheel Skid-Steering Mobile Robot", Int. Journal of Applied Mathematics and Computer Science, Vol. 14, No. 4, pp. 477-496, 2004.

[10] J. Giesbrecht and D. Mackay and J. Collier and S. Verret,"Path Tracking for Unmanned Ground Vehicle Navigation : Implementation and Adaptation of Pure Pursuit",Techinical Memorandum DRDC Suffield TM 2005-224, Dec 2005.

[11] R.C. Coulter,"Implemetation of Pure Pursuit Path Tracking Algorithm", CMU-RI-TR-92-01, Jan. 1992.